Flexible regulation of phase and polarization based on plasma metasurfaces

WEIWEI TAO, YING TIAN, *
Institute of Optoelectronic Technology, China Jiliang University, Hangzhou 310018, China
**Corresponding author: tianyingcjlu@163.com*

Submission: 2026-06-25; Acceptance: 2026-07-17; Publication: 2027-07-31

This paper presents a novel plasma metasurface structure composed of a copper metal patch and a polyimide substrate, operating in the terahertz frequency band (1.6 THz). Based on the Pancharatnam-Berry phase theory, the flexible regulation of the phase and polarization state of light waves has been achieved by optimizing the structural design of subwavelength units. The simulation results show that the designed superlens has a numerical aperture (NA) of 0.6 at a focal length of 1 mm and a half-peak full width (FWHM) of 216 μm. The vortex beam generator can efficiently generate vortex beams with a topological charge number l=1, and the mode purity reaches 0.5. This research provides new ideas for high-frequency tunable photonic devices.

Keywords: Plasma metasurface, geometric phase, terahertz, vortex beam, phase control

1. Introduction

Metasurfaces [1-3] are a new type of two-dimensional planar metamaterials. Compared with traditional metamaterials, they have thinner thickness, higher integration, and lower optical loss [4-5]. Compared with traditional transmission-type phase control devices, metasurfaces demonstrate greater flexibility in phase control, while having a simpler manufacturing process and higher control accuracy. With the spatial resolution capability at the subwavelength scale, metasurfaces can precisely control the electromagnetic wavefront. In addition, its flexible control over characteristics such as polarization states [6-9] and spin Hall effect [10-12]provides a solid technical foundation for the construction of new ultra-thin and highly integrated planar optical and optoelectronic devices [13-14].

Based on the metasurface phase gradient theory, this paper focuses on studying how to precisely control the wavefront phase and polarization of metasurfaces by using geometric phase [15]. Based on the research of metasurfaces, plasma metasurfaces, as an important branch, excite the plasma resonance effect through the subwavelength structure of metals [15-17] or conductive materials, providing an efficient solution for the local regulation of electromagnetic waves. By rationally designing its geometric shape and material combination, plasma metasurfaces can flexibly control the amplitude, phase and polarization of electromagnetic waves, and are widely used in ultra-high resolution imaging, nonlinear optics and high-sensitivity sensing and other fields, demonstrating significant advantages.

As a typical application of metasurface technology, superlenses combine the wavefront regulation capability of subwavelength structures, which can break through the diffraction limit of traditional optical lenses and achieve high-resolution imaging and miniaturized system design. Especially in the fields of optical microscopes and light field

manipulation, superlenses, with their lightweight and multi-functional characteristics, provide significant support for the integrated development of micro-nano optical systems. In addition, the generation of vortex beams [18] combined with metasurfaces further expands its application potential in the field of optics. Vortex beams carry orbital angular momentum (OAM) [19], and their unique helical phase distribution makes them of significant value in the fields of optical capture, optical communication, and quantum information. By designing metasurface unit structures, precise control over the topological charge number and polarization distribution of vortex beams can be achieved, thereby efficiently processing and transmitting multi-dimensional optical information [20-24]. This paper will further explore how to utilize geometric phases to achieve the combination of plasma metasurfaces, superlenses and vortex generators, providing strong theoretical and technical support for the generation of controllable vortex beams.

2. Theoretical Basis

A. Geometric Phase

Geometric phase is a phase effect caused by the variation of the light wave propagation path and its spatial geometric structure. In recent years, it has received extensive attention in the fields of optics and metasurface design. In the design of metasurfaces, the regulation of geometric phase is mainly achieved by precisely designing the geometric shape and spatial arrangement of nanostructures, especially by adjusting the rotation Angle of anisotropic unit structures [25-26]. This phase control method based on rotation Angle has gradually become one of the core fields of metasurface research due to its simple operation and high stability.

The modulation mechanism of geometric phase indicates that when left-handed circularly polarized (LCP) or right-handed circularly polarized light is incident on nanostructures, the phase change of the transmitted light can be described by the following formula:

$$\begin{bmatrix} E_x \\ E_y \end{bmatrix} = \frac{t_i+t_s}{2}\begin{bmatrix} l \\ i \end{bmatrix} + \frac{t_i-t_s}{2} e^{i2\theta}\begin{bmatrix} l \\ -i \end{bmatrix} \quad (1)$$

Among them, t_s and t_i are the normalized complex transmission coefficients of the nanostructure along the long and short axes, respectively. θ represents the rotation Angle of the nanostructure relative to the reference coordinate axis. The phase adjustment of the transmitted light is closely related to the rotation Angle θ, and the geometric properties of the nanostructure directly determine its response characteristics to the polarization state of the incident light. Specifically, the amplitude and phase of the transmitted light can be jointly determined by the complex transmission coefficient, that is, the rotation Angle.

When the nanostructure meets the condition of $t_l = -t_s = l$, the scattering effect caused by the transmission coefficient can be effectively suppressed, and the polarization conversion efficiency can be maximized, thus making the nanostructure behave as an ideal half-wave plate. Under this condition, the change in geometric phase can be expressed by the following formula:

$$\phi = \pm 2\theta \quad (2)$$

In the formula: The positive and negative signs of the symbol correspond respectively to the phase control directions caused by left-handed circularly polarized light (LCP) and right-handed circularly polarized light (RCP). The generation of geometric phase depends on the rotation Angle of the nanostructure, providing a theoretical basis for precisely regulating the phase of incident light. By optimizing the geometric design and rotation Angle of nanostructures, the propagation characteristics of light waves can be efficiently controlled, especially demonstrating excellent performance in the regulation of polarization states and phase distributions. This mechanism has broad application prospects in fields such as metasurface design, polarized light modulation and light field control.

B. Lens Focusing

In optical systems, lenses are important components used to regulate light beams, and their main function lies in focusing the incident light beam to achieve a specific light field distribution. Traditional lenses guide light beams through curved geometric shapes, while metasurface lenses rely on the design of phase gradients to achieve more flexible and precise control of the light field. Compared with traditional optical devices, metasurface lenses have the characteristics of being thin, light, efficient and easy to integrate, which is of great significance in modern optical research.

In order for metasurface lenses to achieve the focusing function, their phase distribution needs to meet specific design requirements. The phase distribution formula of a two-dimensional metasurface lens is as follows

$$\varphi(x,y) = -\frac{2\pi}{\lambda}\left(f - \sqrt{f^2+x^2+y^2}\right) + \Delta\varphi_{n_2} \quad (3)$$

Among them: x, y are the distances from any point on the superlens to the center of the superlens surface (assuming the coordinate of the superlens center is point O, its coordinate is (0,0)), λ is the wavelength of the incident wave, f is the set focal length value, and $\Delta\varphi_{na}$ is the phase compensation value. When the phase distribution conforms to this formula, the superlens can successfully focus the incident light beam at the predetermined position, thereby achieving the optical function.

C. The Generation of Vortex Beams

Vortex beams are a type of beam with a unique wavefront structure, where the wavefront is helical and carries orbital angular momentum (OAM). This characteristic of vortex beams makes them have important applications in fields such as optical communication, quantum information, and optical capture. The core of generating vortex beams based on metasurfaces lies in how to introduce helical phases related to the direction Angle into the light field, so as to produce vortex effects during the beam propagation process. Therefore, its design concept can be generally divided into two schemes: one is the design independent of the polarization state of the incident light, and the other is the design dependent on the polarization state of the incident light.

The first solution is to generate the helical phase $\exp(il\varphi)$ by regulating the geometric characteristics of the metasurface element. Specifically, the geometric parameters of the metasurface unit are adjusted to change its resonant frequency, thereby controlling the phase response of the unit. Through meticulous design, it can be ensured that the phases of different units are fully covered within the range of 0 to 2π. The significant advantage of this method lies in that the phase distribution of the generated vortex beam does not depend on the polarization state of the incident beam [27]. As long as the phase difference between the units remains constant, the helical phase distribution can remain stable. Therefore, this metasurface structure can achieve efficient vortex beam generation under various polarization conditions.

The second scheme is based on the coupling conversion mechanism between spin angular momentum (SAM) and orbital angular momentum (OAM). When circularly polarized light passes through a non-uniform anisotropic medium, its polarization state undergoes orthogonal transformation. This process causes changes in SAM, increasing or decreasing by $\pm\overrightarrow{2\hbar}$. According to the law of conservation of angular momentum, the OAM of the output beam must also compensate for a $\mp\overrightarrow{2\hbar}$ change accordingly [28]. Therefore, for metasurfaces composed of anisotropic units, the phase distribution of the outgoing beam will be supplemented with a helical phase factor $\exp(\pm i2\varphi)$. Since this phase change is generated by the alteration of the beam's polarization state, it is usually referred to as the geometric phase (PB phase) [29], and this chapter implements the vortex beam using the second scheme.

3. The Design of Unit Structure

The design of metasurface unit structures is the basis for achieving specific optical functions. The unit structure designed in this study is composed of rectangular copper metal patches, which are deposited on a polyimide substrate with a lattice constant P of 100 μm and a substrate thickness of 25 μm. The geometric parameters of the rectangular metal patches are 60 μm in length, 20 μm in width, and 0.2 μm in thickness, respectively. As shown in Figure 1, the design of the unit structure takes into account the geometric characteristics at the subwavelength scale to ensure efficient regulation of the light field.

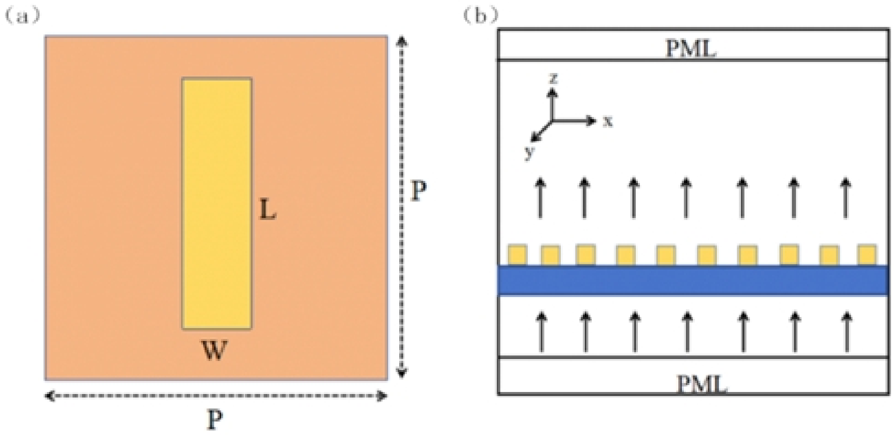

Fig.1. Unit structure schematic diagram:(a)Top view of unit structure;(b)Overall effect drawing.

The transmission performance simulation of the designed unit structure was carried out by using the CST software. The relationship between frequency and transmission efficiency was analyzed by extracting the S parameters. As shown in Fig.2, the transmission efficiency exhibits specific distribution characteristics with frequency, reaching its maximum value around the frequency of 1.6 THz. Therefore, the subsequent research will take 1.6 THz as the working frequency to further optimize and analyze the metasurface performance.

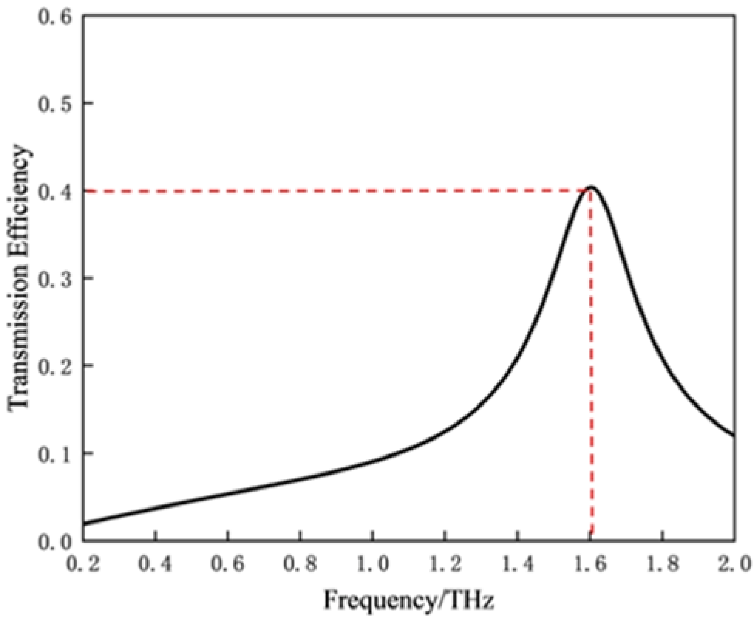

Fig.2. The distribution property of the transmittance of the unit structure varying with frequency.

4. Simulation and Result Analysis

A. Superlens

Focusing lenses play a crucial role in optical systems. By introducing an appropriate phase gradient on the metasurface, incident plane waves can be converted into parabolic waves and focused at the focal point. The phase compensation at each position on the metasurface is

$$F(x) = \frac{2\pi}{\lambda}\left(\sqrt{x^2 + y^2 + f^2} - f\right) \quad (4)$$

In the formula: x and y are the coordinates of the metasurface element structure on the xoy plane, and the center point of the metasurface is (0,0), and f is the preset focal length. In the simulation, the focal length is preset to 1 mm. Fig.3 shows the corresponding superlens model. The lens selected in this chapter uses 15×15 units. As the geometric phase method is mainly adopted, based on the above analysis, the incident light uses circularly polarized light with a frequency of 1.6 THz, which is incident from the Z direction onto the designed structure. The electric field information of the monitor is extracted to analyze the focusing effect of the superlens. Focusing efficiency is one of the important indicators for evaluating the focusing effect of a lens. The commonly used measurement methods are through the half-peak full width FWHM and the numerical aperture NA. To compare the expected effect of the designed superlens with that of the theoretical design, we set the full width of the half-peak as half of the peak height of the focal plane spot to measure the focusing quality of the superlens. The calculation formula is:

$$FWHM = \frac{\lambda}{NA} \quad (5)$$

$$NA = n \sin\alpha \quad (6)$$

Among them: λ is the incident wavelength, NA is the numerical aperture, v is the refractive index of the medium, $\sin\alpha$ is the aperture Angle, and $FWHM$ is the ratio of the radius to the distance from the convergence center. Through calculation, NA=0.6 and $FWHM$=189.4 μm can be obtained.

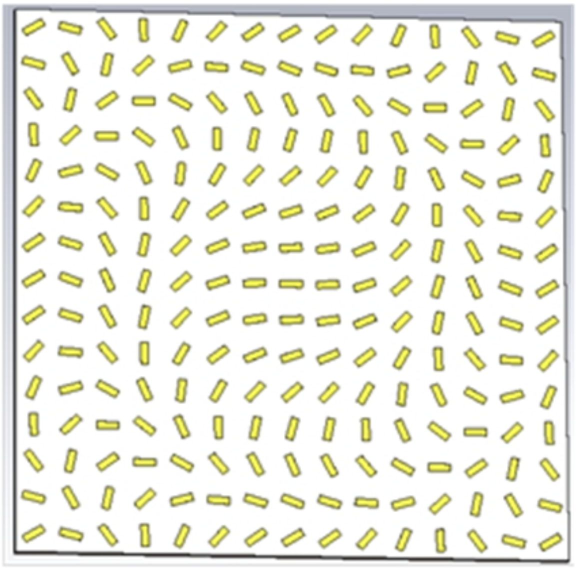

Fig.3. Schematic diagram of superlens.

The focusing effect of the designed superlens is shown in Fig.4. Fig.4 (a) and 4 (c) present the electric field distribution on the x-z and x-y planes respectively. According to Fig.4 (b) of the electric field intensity distribution, it can be found that due to the beam propagating along the negative z direction in the simulation setting, the peak of the electric field intensity is located at -875 μm, but this does not affect the actual function of the superlens. Moreover, it differs by 12.5% in value from the designed focal length of 1000 μm. The X-direction electric field at the focus when y=0 can be obtained as shown in Fig.4 (d). According to the definition of the full width of the half-peak, the FWHM value can be calculated to be 216 μm, which is 12.3% different from the theoretical value of 189.4 μm designed. This result strongly verifies the correctness of the designed superlens theory.

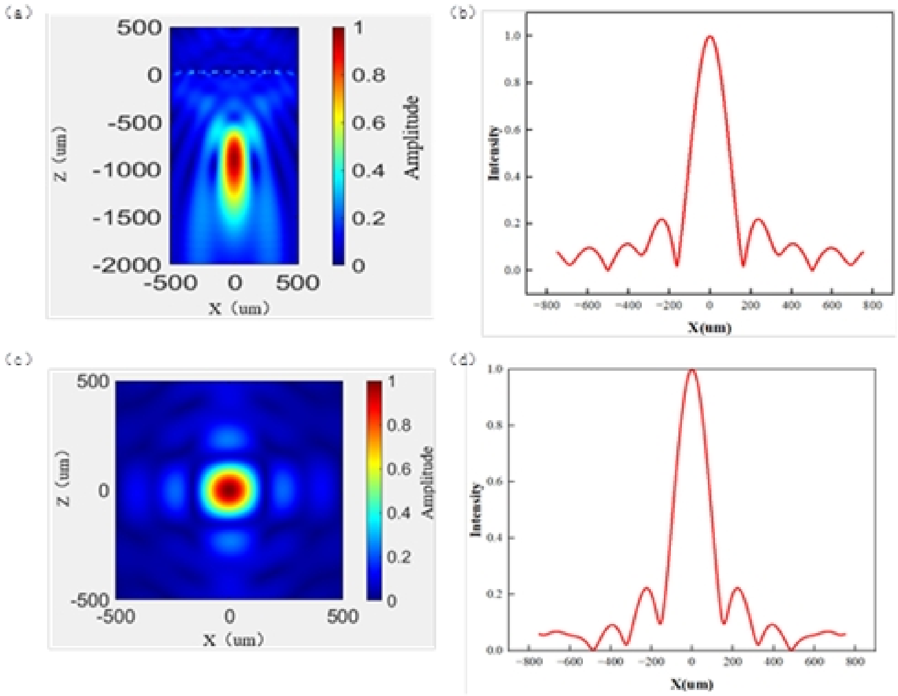

Figure 4 Superlens focusing effect drawing (a) Electric field distribution in the xz plane when y=0; (b) Electric field distribution in the z direction when x=y=0; (c) Electric field distribution in the xy plane when z=0; (d) Electric field distribution in the x direction when y=z=0.

B. Vortex beam generator

Orbital angular momentum is the orbital part of the electromagnetic wave that carries angular momentum, which is generated by the rotation of energy around the optical axis. The wavefront carrying the orbital angular momentum beam is in a vortex shape, so this type of beam is also called a vortex beam. Since the characteristic states of the orbital angular momentum carried by the vortex beam are mutually orthogonal, different modes can provide independent channels for data transmission, thereby enhancing communication performance[30]. In this paper, an orbital angular momentum generator, namely a vortex beam generator, is designed by using the proposed element structure.

The phase distribution of the vortex beam on the cross-section can be expressed as $e^{im\varphi}$, where m and φ are the topological charge number and azimuth, respectively. Vortex beams that can carry orbital angular momentum at specific positions on the metasurface provide compensation phase for the incident beam. Its phase compensation can be expressed as:

$$\varphi_m(x,y) = m\tan^{-1}\left(\frac{x}{y}\right) \quad (7)$$

In the formula, x and y are the coordinates on the metasurface plane respectively. In this paper, a vortex beam generator is designed when the topological charge is equal to 1.

The effect of the designed vortex beam generator is shown in Figure 5. Figure 5 (a) shows the phase compensation distribution and the designed metasurface, while Figure 5 (b) and Figure 5 (c) show the phase distribution and intensity distribution of the generated vortex beam. It can be seen that the phase of the emergent beam carries a spin arm and rotates counterclockwise. The electric field intensity presents a "donut" shape, with the central electric field being 0, which is a characteristic singularity of the vortex beam. The mode purity of the vortex beam was obtained based on the Fourier formula, as shown in Figure 5 (d). Since clockwise is defined as positive, the mode purity of the -1 order (primary mode) that appears is close to 0.5, far exceeding the weights of each order mode, demonstrating excellent benign properties.

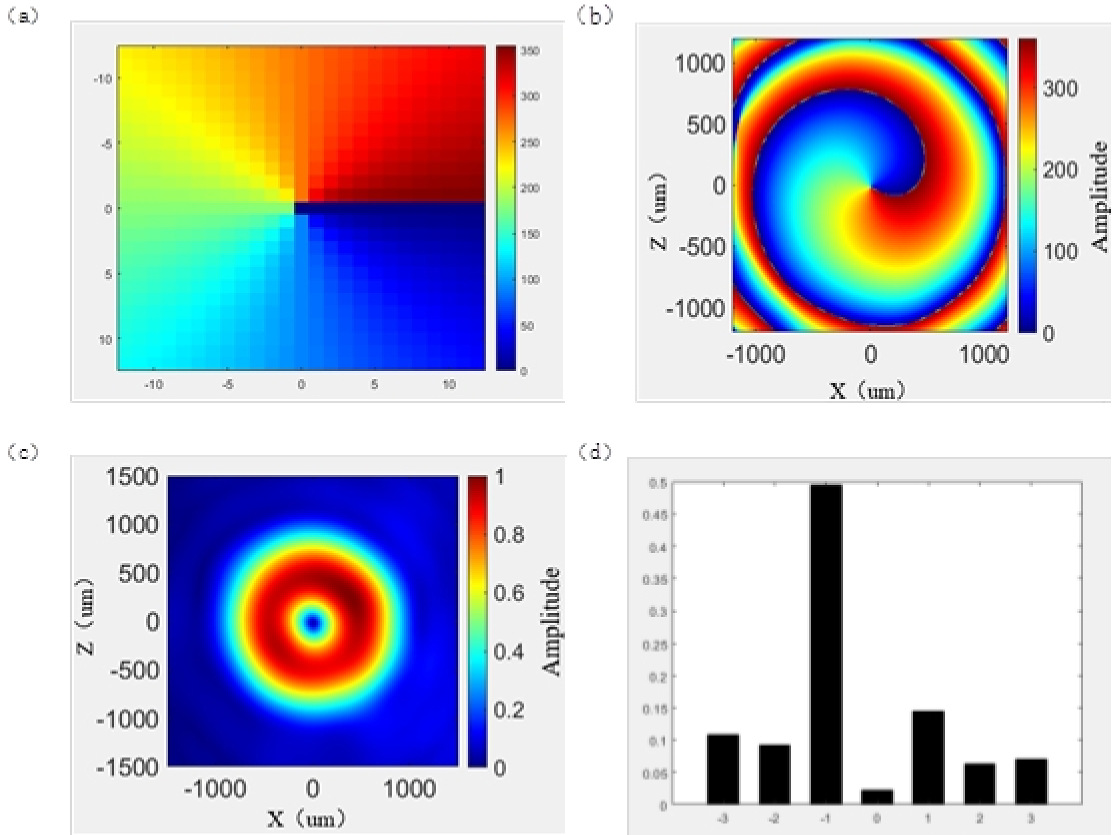

Figure 5 The effect drawing of the vortex beam generator (a) Phase compensation distribution of the vortex beam generator; (b) Phase distribution of the generated vortex beam;(c) intensity distribution of the generated vortex beam;(d) purity of the vortex beam.

5. Summary

Based on the PB phase principle, this paper designs a metasurface unit structure composed of a metal patch and a polyimide substrate. Firstly, the transmission performance simulation is carried out in the 0-2 Thz frequency band to determine the optimal operating frequency. Subsequently, by combining the phase focusing theory of superlenses and the vortex beam generation theory, corresponding metasurface structures were designed respectively, and their optical performance was verified through simulation. The simulation results show that the designed superlens and vortex beam generator have good functional realization capabilities, which proves the feasibility of their design and the correctness of the theory. It also lays the foundation for the subsequent research on tunable perfect vector vortex beam generators.

References

[1] K. Iwaszczuk, A. C. Strikwerda, K. Fan, X. Zhang, R. D. Averitt, P. U. Jepsen, Optics Express **20**(1), 635 (2012).

[2] D. R. Smith, J. B. Pendry, M. C. K. Wiltshire, Science **305**(5685), 788 (2004).

[3] J. B. Pendry, Physical Review Letters **85**(18), 3966 (2000).

[4] J. Shabanpour, Annalen der Physik **532**(10), 2000321 (2020).

[5] X. Zhang, R. Deng, F. Yang, C. Jiang, ACS Photonics **5**(8), 2997 (2018).

[6] B. B. Lake, S. Codeluppi, Y. C. Yung, D. Gao, J. Chun, P. V. Kharchenko, S. Linnarsson, K. Zhang, Scientific Reports **7**(1), 6031 (2017).

[7] J. Li, C. Zheng, J. Li, G. Wang, J. Liu, Z. Yue, X. Hao, Y. Yang, F. Li, T. Tang, Y. Zhang, Y. Zhang, J. Yao, Photonics Research **9**(10), 1939 (2021).

[8] Z. Li, W. Liu, H. Cheng, S. Chen, J. Tian, Scientific Reports **5**(1), 18106 (2015).

[9] Z. Yue, J. Li, C. Zheng, J. Li, M. Chen, X. Hao, H. Xu, Q. Wang, Y. Zhang, J. Yao, Chinese Optics Letters **20**(4), 043601 (2022).

[10] Y. Deng, W. Xu, W. Zhang, Q. Yang, D. Xu, H. Luo, Optics Communications 560, 130480 (2024).

[11] P. Zhao, X. Ding, C. Li, S. Tang, Materials **16**(12), 4259 (2023).

[12] Z. Ma, Z. Lai, S. Lin, J. Hong, Y. Chen, X. Zhou, Optics Letters **48**(11), 3003 (2023).

[13] M. Kang, J. Chen, X. L. Wang, H. T. Wang, J. Opt. Soc. Am. B **29**(4), 572 (2012).

[14] X. Ding, F. Monticone, K. Zhang, L. Zhang, D. Gao, S. N. Burokur, A. de Lustrac, Q. Wu, C. W. Qiu, A. Alù, Advanced Materials **27**(7), 1195 (2015).

[15] W. Sichak, D. J. Levine, Proceedings of the IRE **43**(11), 1661 (1955).

[16] Y. Zhang, M. Pu, J. Jin, X. Lu, Y. Guo, J. Cai, F. Zhang, Y. Ha, Q. He, M. Xu, X. Li, X. Ma, X. Luo, Opto-Electronic Advances **5**(11), 220058 (2022).

[17] Z. Yue, J. Li, J. Li, C. Zheng, J. Liu, G. Wang, H. Xu, M. Chen, Y. Zhang, Y. Zhang, J. Yao, Opto-Electronic Science **1**(3), 210014 (2022).

[18] Q. Zhao, S. Tu, Q. Lei, C. Guo, Q. Zhan, Y. Cai, Photonics Research **10**(7), 1617 (2022).

[19] L. Allen, M. W. Beijersbergen, R. J. C. Spreeuw, J. P. Woerdman, Physical Review A **45**(11), 8185 (1992).

[20] Y. Bao, J. Ni, C. W. Qiu, Advanced Materials **32**(6), 1905659 (2020).

[21] Y. Zhang, W. Liu, J. Gao, X. Yang, Advanced Optical Materials **6**(4), 1701228 (2018).

[22] S. Chen, Z. Xie, H. Ye, X. Wang, Z. Guo, Y. He, Y. Li, X. Yuan, D. Fan, Light: Science & Applications **10**(1), 222 (2021).

[23] H. Zhao, X. Wang, S. Liu, Y. Zhang, Opto-Electronic Advances **6**(2), 220012 (2023).

[24] S. J. Li, Y. B. Li, L. Zhang, Z. J. Luo, B. W. Han, R. Q. Li, X. Y. Cao, Q. Cheng, T. J. Cui, Laser & Photonics Reviews **15**(2), 2000449 (2021).

[25] M. V. Berry, Journal of Modern Optics **34**(11), 1401 (1987).

[26] S. Pancharatnam, Proc. Indian Acad. Sci. A 44, 247 (1956).

[27] H. Rubinsztein-Dunlop, A. Forbes, M. V. Berry, M. R. Dennis, D. L. Andrews, M. Mansuripur, C. Denz, C. Alpmann, P. Banzer, T. Bauer, E. Karimi, L. Marrucci, M. Padgett, M. Ritsch-Marte, N. M. Litchinitser, N. P. Bigelow, C. Rosales-Guzmán, A. Belmonte, J. P. Torres, T. W. Neely, M. Baker, R. Gordon, A. B. Stilgoe, J. Romero, A. G. White, R. Fickler, A. E. Willner, G. Xie, B. McMorran, A. M. Weiner, Journal of Optics **19(**1), 013001 (2017).

[28] L. Marrucci, C. Manzo, D. Paparo, Physical Review Letters **96**(16), 163905 (2006).

[29] R. C. Devlin, A. Ambrosio, N. A. Rubin, J. P. B. Mueller, F. Capasso, Science **358**(6365), 896 (2017).

*Corresponding authors: tianyingcjlu@163.com